IOP Conf. Series: Materials Science and Engineering **101** (2015) 012058 doi:10.1088/1757-899X/101/1/012058

New measurements of multilayer insulation at variable cold temperature and elevated residual gas pressure

Th Funke and Ch Haberstroh

Technische Universitaet Dresden, Bitzer-Stiftungsprofessur fuer Kaelte-, Kryo- und Kompressorentchnik, Dresden, 01062, Germany

E-mail: thomas.funke@tu-dresden.de
christoph.haberstroh@tu-dresden.de

Abstract. New MLI measurements at the TU Dresden flow type calorimeter have been carried out. Specimens of 20 layer double side aluminized polyester film were tested. A cylindrical cold surface of 0.9 m² is held at the desired cold boundary temperature between approximately 30 K and 300 K. The heat transfer through the MLI is measured by recording the mass flow as well as the inlet and the outlet temperature of the cooling fluid. Measurements at varied cold boundary temperatures have been performed. Moreover the effect of an additional vacuum degradation – as it might occur by decreasing getter material performance in real systems at elevated temperatures – is studied by a controlled inlet of nitrogen gas. Thus the vacuum pressure was varied over a range of 10^{-7} mbar to 10^{-2} mbar. Different cold boundary temperatures between 35 K and 110 K were investigated. Test results for 20 layer MLI are presented.

1. Introduction

A calorimeter cryostat at TU Dresden allows performing MLI measurements at variable cold temperature and elevated vacuum pressure.

MLI under high vacuum conditions is naturally most effective. But the operational temperature e.g. in cryo-compressed storage vessels using MLI in vacuum insulation – currently investigated for automotive hydrogen storage solutions [1] – stretches out from 30 K up to 300 K. MLI performance data for such a wide temperature span are not available to date. The vacuum insulation of a CcH2 storage vessel for automobiles degrades gradually over its operating time. Additional vacuum degradation caused by decreasing getter material performance at elevated temperatures can be simulated and studied by a controlled inlet of e.g. nitrogen gas.

2. Conceptual design and setup

It was reported earlier about the detailed conceptual cryostat design in [2]. The test setup is slightly modified by means of additional temperature sensors for monitoring purpose. Major improvements are achieved by the test procedure itself and an extended data analysis.

It is a flow type cryostat. The MLI is mounted on a test cylinder. The effective area is confined by the cylindrical part of this test area. Preferably liquid helium (LHe) respectively helium cold gas is used as a cooling fluid to hold the test cylinder at the desired temperature.

An external heater can preheat the fluid in order to achieve the desired temperature for the test cylinder. The integral value of the heat load on this test cylinder is measured. It is predominated by the

heat flux through the MLI, plus some minor, inevitable parasitic heat fluxes. The chosen geometries and dimensions allow measurements for various MLI layouts, mounting techniques and test conditions. During operation the cooling fluid is led through the cryostat, cooling the test cylinder and all thermal shields. Before coming into contact with the test cylinder, the inlet flow is heated up to a temperature T_1 by means of a controlled external heater. The isothermal test cylinder is kept at a slightly higher preselected operating temperature T_2 by this cryogenic fluid flow during the whole measurement.

The heat load onto the test cylinder then can be easily and quite precisely derived from cooling fluid mass flow, its heat capacity and the temperatures T_1 and T_2:

$$\dot{Q} = \dot{m} \cdot \int_{T_1}^{T_2} c_p dT \tag{1}$$

$$\dot{q} = \frac{1}{A} \cdot \dot{m} \cdot \int_{T_1}^{T_2} c_p dT \tag{2}$$

with (1) standing for the total heat load in [W] and (2) standing for the area specific heat load in [W/m²].

The instrumentation is primarily designed for He cold gas as cooling fluid. Nonetheless - especially at higher temperatures - nitrogen will be used alternatively. The cold gas mass flow at the calorimeter outlet is passively warmed up to ambient temperatures. A precise control valve and a flow meter are following downstream.

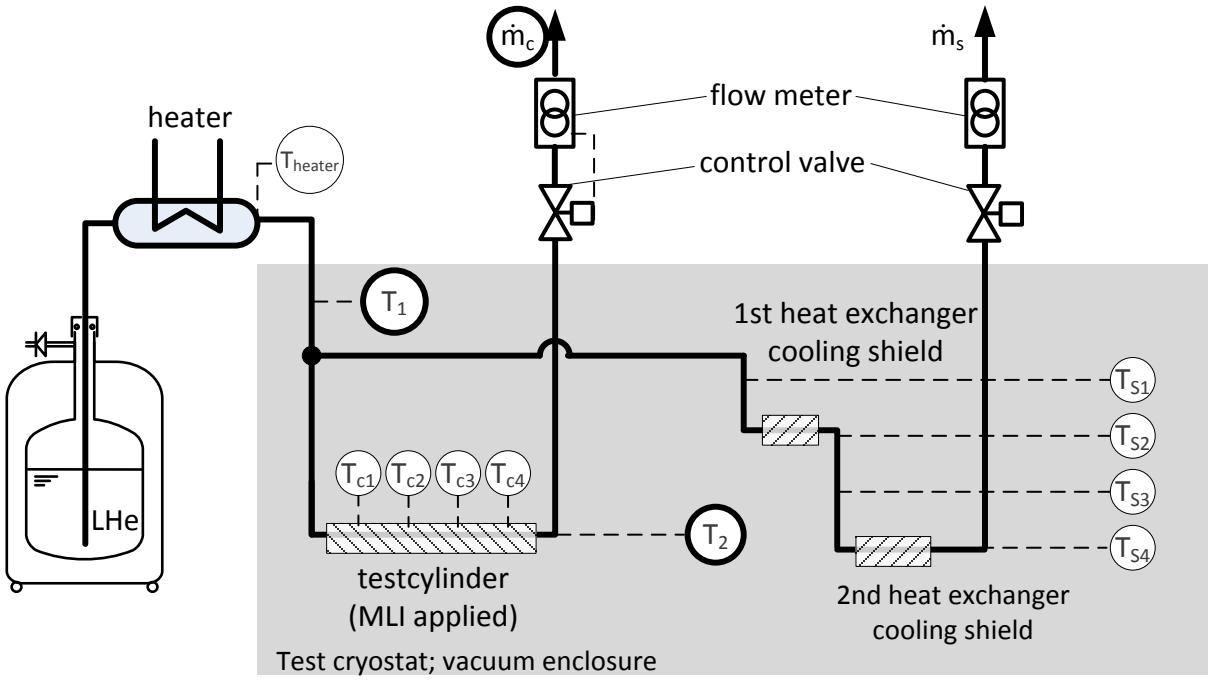

Figure 1. Design of the flow cryostat with LHe supply, external heater and the cryostat itself. T_1, T_2 and $\dot{m}_c$ are the measured values used for the heat load determination

Besides the variable cold temperature, gravimetric effects on the thermal performance of the MLI shall be investigated. Therefore the cryostat is designed for operation in tilted orientation as well. All ducts and connections are mounted in a way to allow an inclination up to 90°.

Some examples for typical parameters at two different operating points are presented using the fluid database [4]. In these calculations two mass flows of 0.05 g/s and 0.03 g/s with helium as cooling fluid are considered. The heat flux through the MLI is assumed to account for $\dot{\mathbf{q}}$ = 1 W/m^2 according to [6]. The cryostat is primarily designed for helium as cooling fluid. Alternatively, i.e. for higher surface temperatures, nitrogen can be used. The measurements are carried out under high vacuum conditions or at defined degraded vacuum conditions. Therefore a needle valve is installed to vent the vacuum space with small amounts of a preselected gas. Figure 2 shows the mean apparent thermal conductivity to be expected for various MLI for different vacuum conditions. The data is a compilation from literature to be found in [5].

Besides the variable cold temperature and residual gas pressure, gravimetric effects on the thermal performance of the MLI shall be investigated. Therefore the cryostat is designed for operation in tilted orientation as well. All ducts and connections are mounted in a way to allow an inclination up to 90°.

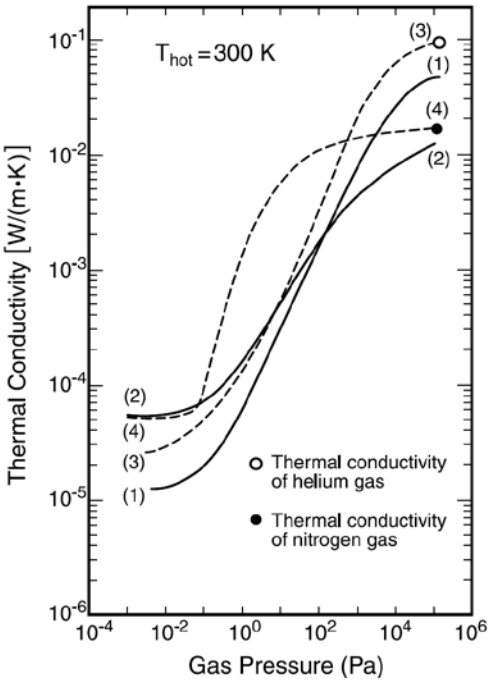

Figure 2. Mean apparent thermal conductivity of various multilayer insulation (MLI) as a function of gas pressure in a vacuum space, with a hot-wall temperature T_{hot} = 300 K. The MLI is composed of aluminized Mylar layers separated by various insulating spacer layers: (1) Al foil + fiberglass paper (with residual helium gas in the vacuum space) and a cold-wall temperature Tcold = 20 K; (2) Al foil + fiberglass paper (with residual nitrogen gas) Tcold = 77 K; (3) double-aluminized Mylar double-aluminized Mylar (NRC-2) (with nitrogen gas) T_{cold} = 79 K. (Compiled by Nast 2000 from data in Little 1963, Lockheed 1964, and Boberg 1964.) [5]

The calorimeter is of concentrical cylinder type and is tiltable from vertical to horizontal orientation. All inner parts are mounted at the top flange of the cylindrical vacuum vessel (Figure 3). The cold cylinder is suspended on top and bottom via GFRP rods. The vacuum jacket represents the warm boundary. The major components and their dimensions are as follows: The cold cylinder is made of 219 mm outer diameter,1300 mm long and 3 mm thick seamless copper pipe. Which yields to a outer surface of 0.89 m^2. The whole surface area is nickel plated and high gloss polished to reduce the emissivity on the outer surface. On the upper and lower ends are thermal shields to minimize undesired heat loads. Each shield is actively cooled via the preconditioned cooling fluid. The first heat exchanger is mounted on the top shield the second on the lower end. They are connected in series. Two Si-Diodes with a accuracy of 250 mK up to 100 K are installed. This two sensors are CU package and in four wire configuration. A total of 10 standard Pt100 temperature sensors are installed for monitoring purpose as well. Sensor number Tc1 . . .Tc4 are mounted on the inside of the test cylinder to check for isothermal conditions. They are mounted according to the manufacturer standards in a copper bobbin. All wires are thermally anchored at the upper radiation shield.

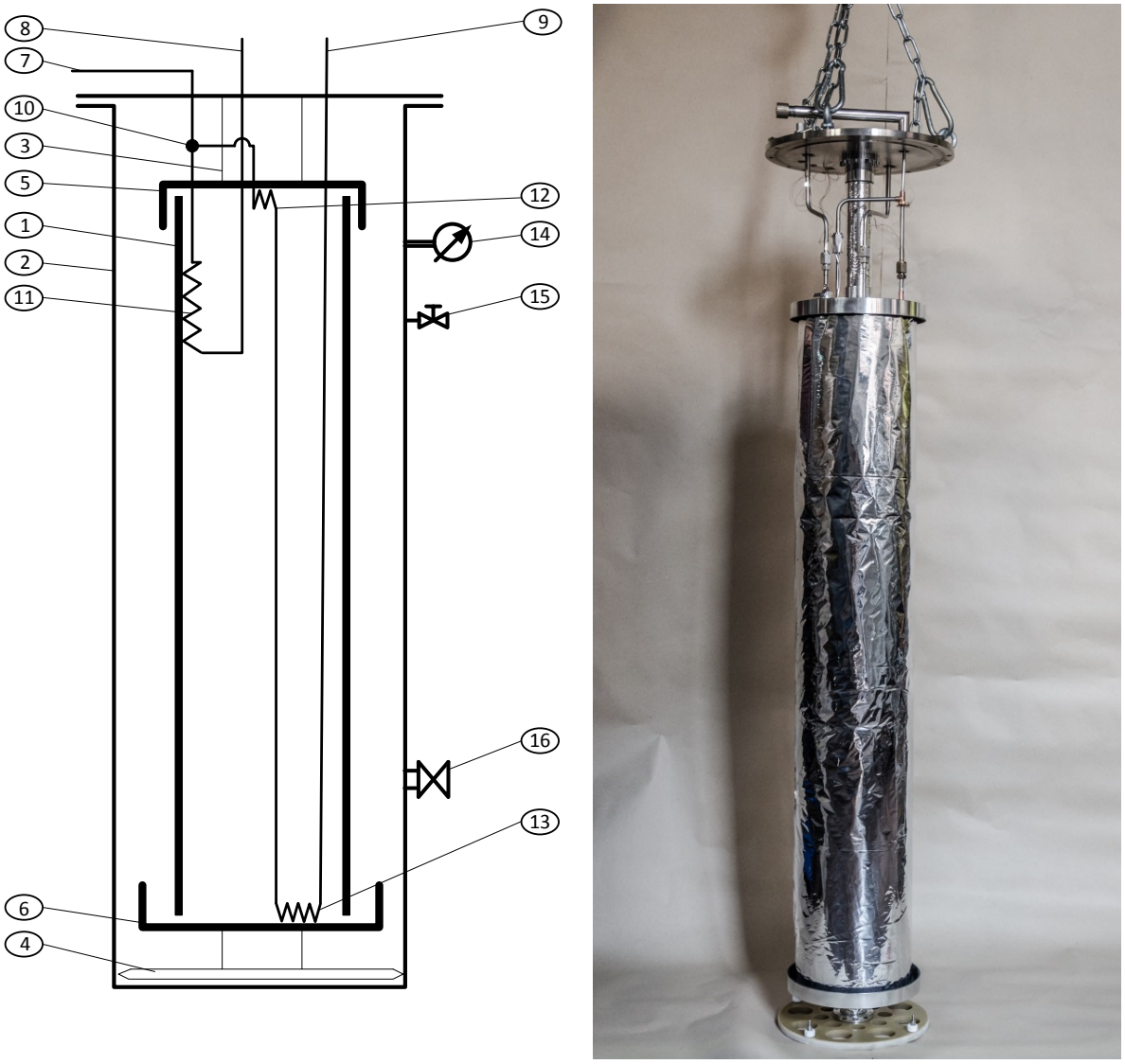

Figure 3. left: Scheme of the calorimeter: 1- cold cylinder, 2 - warm cylinder, 3 - upper support rod, 4 - lower support rod, 5 - upper radiation shield, 6- lower radiation shield, 7 - cooling fluid inlet, 8 - cooling fluid test cylinder out, 9 – shield cooling out, 10 - T-section of inlet line, 11 - heat exchanger test cylinder, 12 - 1st heat exchanger shield ccooling, 13 - 2nd heat exchanger shield cooling, 14 - vacuum gauge, 15 - needle valve, 16 - vacuum port; **right:** photo of the upper and lower part of the cryostat, MLI wrapped around the test cylinder

There are two heat exchangers to cool the shield and the support structure. Their inlet and outlet temperature is measured and represented by TS 1...TS 4. The external heater uses another two sensors, where T_{heater} is the set temperature. The helium dewar is externally pressurized at a constant level of 1.5 bar absolute pressure. The mass flow through the test cylinder is controlled by a Bronkhorst F-112AC flow meter and a control valve type F-004AC-LUU-49-V from the same manufacturer. The mass flow of the shield circuit is adjusted manually and a thermal mass flow meter type Sierra ML100 is used to measure the flow rate. Both flow meters are placed at ambient temperature of about 21 °C. The data acquisition system consists of a LakeShore 224 temperature monitor and a thyristor controller built by CryoVac (Germany) using a Eurotherm controller unit for the external electrical heater. A turbomolecular pump is used to maintain a proper vacuum inside the cryostat of about

10^{-5} mbar, unless intentional gas is injected to degrade the vacuum to a certain level. A wide range vacuum gauge type Pfeiffer PKR 251 is mounted on the upper part of the cryostat.

Table 1. Uncertainties for the temperature sensors and the mass flow meter

	T_1 and T_2	Mass flow meter
Type	DT-670A	0.05 g/s
Manufacturer	LakeShore	Bronkhorst
Tolerance bands /Accuracy	2 K to 100 K: ±0.25 K 100 K to 305 K: ±0.5 K	0.5 %Reading + 0.1 full scale (calibrated at 20 °C and 1.5 bar)

3. Test procedure and experimental data

The MLI sample (20 layer double side aluminized mylar, type RUAG CoolCat 2NW) is wrapped around the test cylinder in vertical orientation. It is butt joined and the gap is covered by one layer of aluminium tape (Figure 4). The calorimeter is then placed inside the vacuum vessel. The insulation space is evacuated utilizing a turbomolecular pump. After 12 – 24 h a pressure of 10^{-5} mbar is achieved. Meanwhile a LHe dewar is connected via vacuum insulated transferline to an also vacuum insulated external heater which is connected to the cryostat inlet.

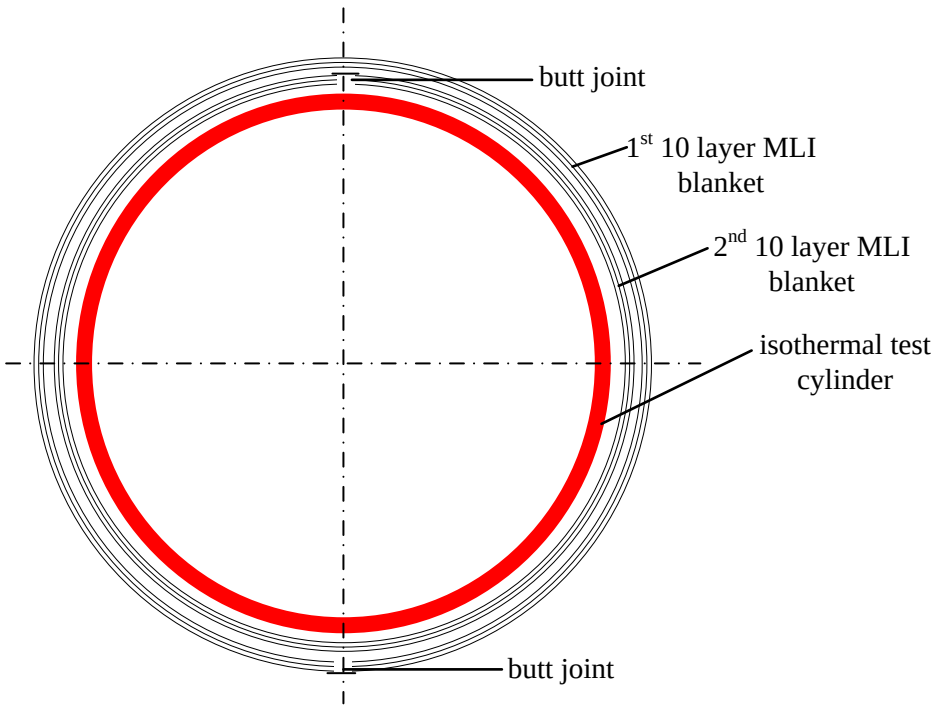

Figure 4. Sketch of the insulation cross section. Two MLI blankets of 10 layer each are wrapped around the test cylinder. The blankets are butt joined and the gap is covered by one layer of aluminium tape

For a fast cooldown high mass low rates up to 0.2 g/s are set. The temperature controller to heat up the inlet stream is brought in line when the desired cold temperature of the test cylinder is achieved. Using an estimated value for the total heat load, the inlet temperature T_1 is precalculated and set by the external heater. The cylinder temperature T_2 adapts very slowly. Hence the inlet temperature is

adjusted according to the temperature slope of the test cylinder manually in adaption of the gradient of T_2.

To degrade the vacuum level pure nitrogen gas is led into the vacuum space using a fine needle valve. Measurements at three constant vacuum levels are carried out - high vacuum 10^{-7} mbar, 10^{-3} mbar and 10^{-2} mbar.

Figure 5 shows a typical test run at high vacuum conditions. The mass flow is changed during operation from 0.05 g/s to 0.033 g/s and the temperature T_1 is adapted to keep the test cylinder temperature constant. The time plot shows the complete test starting with the cool down from room temperature using high helium mass flow. After roughly 2 h the test cylinder is at the desired temperature and the cooling fluid mass flow is reduced. The total heat load is calculated at 3 discrete moments (see table 2) were steady state conditions are achieved. During operation the LHe dewar needs to be changed several times, at about 510 min, 1200 min and 1370 min indicated by a full stop of the He mass flow.

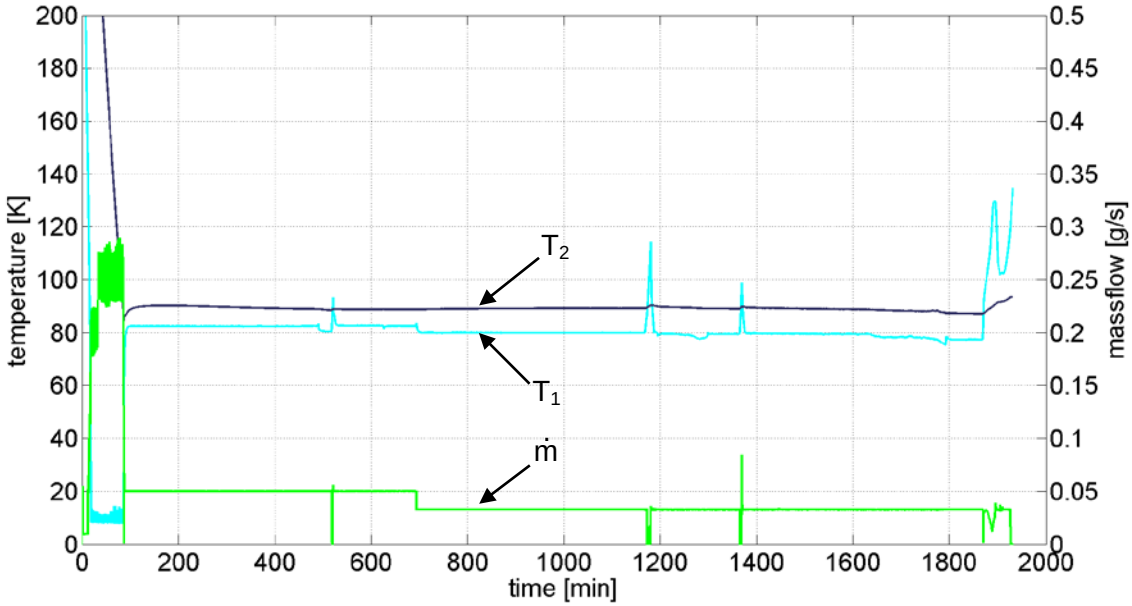

Figure 5. Sketch of the insulation cross section. Two MLI blankets of 10 layer each are wrapped around the test cylinder. The blankets are butt joined and the gap is covered by one layer of aluminium tape

Table 2. Experimental data of one experiment, 20 layer double side aluminized mylar MLI; test cylinder inlet and outlet temperature and shield cooling , vacuum pressure 10^{-7} mbar

T_1 [K]	T_2 [K]	$\dot{m}$ [g/s]	Upper radiation shield [K]	Lower radiation shield [K]	Heat load $\dot{Q}$ [W]
82.7	88.8	0.05 g/s	94.4	104.8	1.58
82.6	88.7	0.05 g/s	92.5	101.8	1.61
79.9	89.2	0.033 g/s	89.1	101.3	1.60

4. Analysis

Further experiments were carried out and are summarized in Figure 6. The diagram shows the total heat load onto the test cylinder over cold boundary temperature for vacuum pressure at 10^{-7} mbar, 10^{-4} mbar, 10^{-3} mbar and 10^{-2} mbar. All calculated heat loads are an average of multiple measurements, or averaged over a period of 10 min in steady state condition. A slope of T_2 (test cylinder outlet temperature) of less than ($3\ 10^{-2}$ K/10 h) is set as steady state criteria.

The total heat load rises significantly at a residual gas pressure of 10^{-3} mbar. From 10^{-7} to 10^{-4} mbar no major changes are observed. Graph 2 in Figure 2 shows an slowly increasing thermal conductivity at 10^{-2} Pa, 10^{-4} mbar respectively and a strong slope at 10^{-1} Pa (10^{-3} mbar). Matching to this a significant increase in the measured heat loads at 10^{-3} mbar is observed. For better comparison to Figure (2) the apparent thermal conductivity at cold temperature of about 77 K is calculated using equation (3) with a thickness of δ=3.5 mm and a warm temperature of 294 K. As shown in Table 3 the k-value is more than doubled from 10^{-7} mbar to 10^{-3} mbar. Graph (2) in figure (2) rises about the same within this range. This is a brief comparison using vacuum pressure within the given order of magnitude. Especially at degraded vacuum conditions a more detailed investigation is necessary.

.

$$k = \dot{q} \cdot \frac{\delta}{\Delta T} \tag{3}$$

Table 3. Apparent thermal conductivity at high vacuum conditions and degraded vacuum; (warm boundary temperature 294 K)

Cold boundary temperature	Vacuum pressure	k-value
79.9 K	10^{-7} mbar (10^{-5} Pa)	$2.5\ 10^{-5}$[W/mK]
65.9 K	10^{-4} mbar (10^{-2} Pa)	$2.7\ 10^{-5}$[W/mK]
77.7 K	10^{-3} mbar (10^{-1} Pa)	$5.5\ 10^{-5}$[W/mK]
118.1 K	10^{-2} mbar (1 Pa)	$20.7\ 10^{-5}$[W/mK]

A first approximation of the uncertainty of the measurements resulting from the uncertainty of the temperature sensors and the flow meter is given in equation (3) were the error propagation of three independent variables T_1, T_2 and m is applied. The specification for the mass flow meter and the temperature sensors are given in section 3. The calculation using equation (4) in (1) leads to uncertainties of 7 % in best case to 15 %. This range depends on the measurement conditions, governed by the working range of the mass flow meter. This analysis neglects any parasitic loss through the support structure and edge effects on both ends. Therefor it is subject for further investigations in order to characterize the calorimeter.

$$\Delta\dot{Q} = \sqrt{\left(\frac{\partial \dot{Q}}{\partial T_1}\right)^2 \cdot \Delta T_1^2 + \left(\frac{\partial \dot{Q}}{\partial T_2}\right)^2 \cdot \Delta T_2^2 + \left(\frac{\partial \dot{Q}}{\partial \dot{m}}\right)^2 \cdot \Delta \dot{m}^2} \tag{3}$$

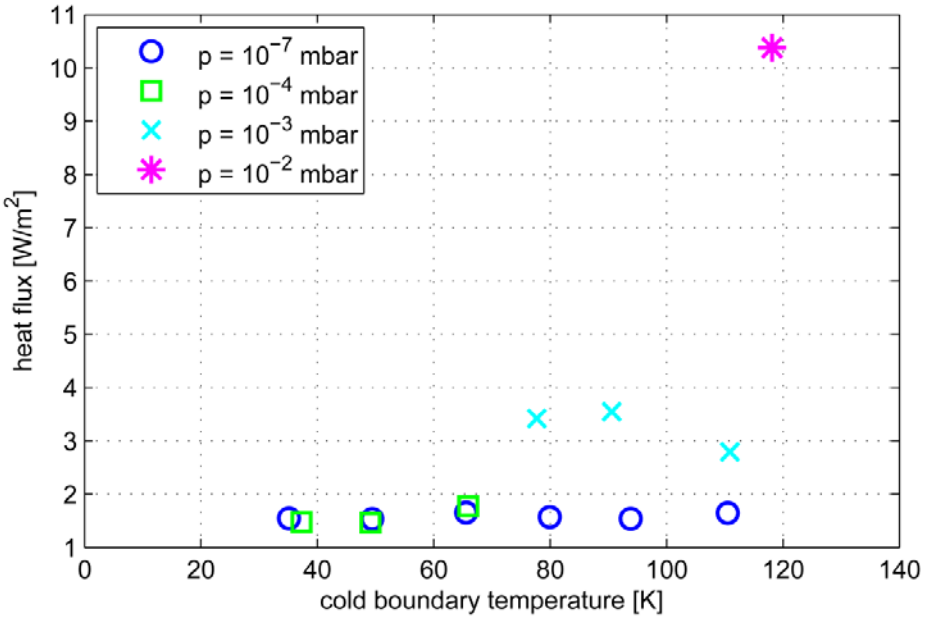

Figure 6. Heat flux through 20 layer MLI vs. cold boundary temperature at vacuum pressure of 10^{-7} mbar, 10^{-4} mbar, 10^{-3} mbar and 10^{-2} mbar

5. Conclusion and outlook

A number of measurements to characterize a 20 layer MLI at variable cold boundary temperature and elevated gas pressure were carried out. The test procedure and the data analysis are widely standardized. A comparison of these results to existing correlations such as the Lockheed equation or the layer by layer model [4] is subject of the upcoming work.

The intended measurements in horizontal orientation in order to detect any gravimetric degradation in the thermal performance of the same MLI will follow after a detailed error analysis including sensor accuracy and parasitic heat flux such as solid conduction from the support structure in order to characterize the calorimeter.

6. References

[1] Aceves S M, Brunner T C, et al. 2010 High-density automotive hydrogen storage with cryogenic capable pressure vessels *Int. J. of Hydrogen Energy vol 35 ed T N Veziroglu (Miami Fl Elsevier) issue 3 pp 1219-1226*

[2] Funke Th and Haberstroh Ch 2014 A calorimeter for measurements of multilayer insulation at variable cold temperature *ICEC Twente Preprint gr-qc/0401010*

[3] Lemmon E R, Huber M L and McLinden M O 2013 NIST Standard Reference Database 23 Reference Fluid Thermodynamic and Transport Properties-REFPROP Version 9.1

[4] McIntosh G 1994 Layer by Layer MLI Calculation Using a Separated Mode Equation *Advances in Cryogenic Engineering* **39B** 1683

[5] Ekin J W 2011 *Experimental techniques for Low-Temperature Measurements* Oxford University Press

[6] Lehmann W, 2000 *Superisolation (SI) deren Qualitaet und Degradierung bei Anwendungen in der Kryotechnik DKV-Tagung, Bremen*